ORIGINAL ARTICLE

doi:10.1111/evo.14614

Evolutionary rates and shape variation along the anuran vertebral column with attention to phylogeny, body size, and ecology

Katie A. Adler,[1] Diego L. De Nault,[1] Cassandra M. Cardoza,[1] and Molly Womack[1,2,3]

[1]*Museum of Vertebrate Zoology, University of California, Berkeley, Berkeley, California 94720*

[2]*Department of Biology, Utah State University, Logan, Utah 84322*

[3]*E-mail: molly.womack@usu.edu*

Received March 3, 2022

Accepted August 8, 2022

The vertebral column is critical to a vertebrate species' flexibility and skeletal support, making vertebrae a clear target for selection. Anurans (frogs and toads) have a unique, truncated vertebral column that appears constrained to provide axial rigidity for efficient jumping. However, no study has examined how presacral vertebrae shape varies among anuran species at the macroevolutionary scale nor how intrinsic (developmental and phylogenetic) and extrinsic (ecological) factors may have influenced vertebrae shape evolution. We used microCT scans and phylogenetic comparative methods to examine the vertebrae of hundreds of anuran species that vary in body size as well as adult and larval ecology. We found variation in shape and evolutionary rates among anuran vertebrae, dispelling any notion that trunk vertebrae evolve uniformly. We discovered the highest evolutionary rates in the cervical vertebrae and in the more caudal trunk vertebrae. We found little evidence for selection pressures related to adult or larval ecology affecting vertebrae evolution, but we did find body size was highly associated with vertebrae shape and microhabitat (mainly burrowing) affected those allometric relationships. Our results provide an interesting comparison to vertebrae evolution in other clades and a jumping-off point for studies of anuran vertebrae evolution and development.

KEY WORDS: **Allometry, evolutionary rate, microhabitat, modularity, presacral vertebrae.**

The vertebral column strongly influences flexibility and skeletal support (Long et al. 1997; Schilling 2011; Rawls and Fisher 2018) and presacral vertebrae variation arose as tetrapod species diversified in size and ecology (Müller et al. 2010). Some clades vary drastically in presacral vertebrae number, for example, squamates (lizards and snakes) range from 14 to over 300 trunk vertebrae (Bergmann and Irschick 2012) and caudata (newts and salamanders) range from 12 to 61 trunk vertebrae (Bonett and Blair 2017). In contrast, mammals are conserved or constrained in vertebrae number (most species have seven cervical and 19 trunk vertebrae [Narita and Kuratani 2005; Müller et al. 2010; Asher et al. 2011]), but show substantial interspecific variation in vertebrae size and shape related to body size and locomotion type (Randau et al. 2016; Randau and Goswami 2017; Jones et al. 2018b). Like mammals, anurans are conserved in presacral vertebrae number; however, it is unclear if anuran vertebral shape varies in region-specific ways in relation to species ecology or body size, as in mammals (Randau et al. 2016, 2017; Randau and Goswami 2017; Jones et al. 2018b).

The anuran (frog and toad) presacral vertebral column appears uniquely constrained to provide axial rigidity for efficient jumping (Emerson 1985; Handrigan and Wassersug 2007); however, the relative influence of intrinsic (developmental and phylogenetic) and extrinsic (ecological) factors on anuran vertebrae evolution remains unexamined. More closely related species often share more similar genetic and developmental pathways that could intrinsically influence the evolution of anuran posterior presacral vertebrae in association with phylogeny. Alternatively,

extrinsic factors such as selection pressures related to locomotion could play a dominant role in the evolution of anuran vertebrae. The majority of anuran species have only one cervical vertebra and four to eight trunk vertebrae (Handrigan and Wassersug 2007). Because the anuran vertebral column is so truncated, it may lack the modularity that facilitates mammalian vertebrae shape adaptation to ecological and locomotor selection pressures. High modularity is indicated by more independent evolution (less covariation) among vertebrae, such as the subdivision of mammalian trunk vertebrae into thoracic and lumbar regions, allowing mammalian vertebrae sections to modularly (more independently) evolve different functional roles related to ecology and locomotion (Randau et al. 2016; Randau and Goswami 2017; Jones et al. 2018a,b). Although phylogenetic variation in presacral vertebrae form has been described (Nicholls 1916; Noble 1922; Mookerjee and Das 1939; Ritland 1955; Zweifel et al. 1956; Griffiths 1963; Emerson 1982; Cannatella and Trueb 1988a,b; Maglia 1998; Baez et al. 2000; Blanco and Sanchiz 2000; Pramuk 2002; Pugener 2002; Fabrezi 2006; Pramuk 2006), no studies have examined tvertebrae shape at the macroevolutionary scale, leaving little understanding of whether presacral vertebrae evolution varies along the vertebral column or if particular vertebrae are more influenced by intrinsic factors or extrinsic factors.

Although many aspects of the overall anuran skeleton shape have diversified based on adult microhabitat, it remains unknown if adult microhabitat has influenced vertebrae shape evolution. Adult anurans live in a variety of microhabitats (e.g., aquatic, arboreal, burrowing, and terrestrial; Moen and Wiens 2017) that require different locomotor strategies (swimming, walking, climbing, etc.; Buttimer et al. 2020) and likely different demands on axial bending and rigidity. For example, salamanders with aquatic-only life cycles have increased numbers of trunk vertebrae and elongate bodies to assist with undulation through water (Bonett and Blair 2017), aquatic and semi-aquatic crocodylomorph taxa have relatively broad transverse processes that increase the leverage of lateral flexors (Molnar et al. 2015), and sirenians (dugongs and manatees) have compressed cervical and elongate thoracic vertebrae, shortened neural spines, and other vertebrae modifications that aid in caudal aquatic propulsion (Reidenberg 2007). Although aquatic anurans do not have particularly elongate bodies, selection pressure for increased swimming performance (Moen 2019) may influence vertebrae shape evolution. Burrowing may also influence vertebrae shape, as burrowing imposes strong selection pressure on other anuran skeletal features thought to aid in moving underground, including limbs (Moen et al. 2013; Vidal-García and Scott Keogh 2017; Keeffe and Blackburn 2020; Stepanova and Womack 2020), digits, (Moen et al. 2013), and skulls (Vidal-García and Scott Keogh 2017; Bardua et al. 2021). Specifically, burrower posterior presacral vertebrae may have decreased relative transverse processes lengths, because pelvic sacral distal expansion is found in burrowing and walking species (Emerson 1982; Buttimer et al. 2020) and decreased relative lengths of posterior presacral vertebrae transverse processes prevent interference with the anteroposterior sliding of the ilia (Emerson 1982). Finally, anurans may mirror felids and show changes in vertebrae shape associated with arboreality or climbing when compared to terrestrial species (Randau et al. 2016; Jones et al. 2018b).

Larval habitat could also influence the evolution of vertebrae shape because vertebrae begin developing and ossifying prior to metamorphosis (Analía Púgener and Maglia 1997; Haas 1999; Wild 1999; Zhang et al. 2021). Although the vertebral column has been characterized as relatively short and inflexible in most anuran adults, it participates in left-right lateral bending in free-swimming anuran larvae (tadpoles), which generates thrust during undular movement (Azizi et al. 2007). Species that inhabit lotic conditions, where the flow of water can act as a pressure against forward movement, may exhibit differences in the shapes of their vertebrae compared to species inhabiting lentic conditions. Furthermore, if vertebrae shape is influenced by larval swimming behavior, then species that develop directly to their adult morphology within an egg would face less selection pressure on vertebral shape related to the larval phase. Thus, vertebrae may be subjected to unique pressures depending on the environment in which they develop (lentic habitat, lotic habitat, or within-egg direct development).

Variation in developmental timing within the vertebral column may also influence anuran vertebrae evolutionary rates. In anurans, earlier developing structures are often found to be more evolutionarily constrained than later developing structures, as seen in skulls (Bardua et al. 2021) and limbs (Stepanova and Womack 2020). Anuran vertebral development begins with the neural arches, which develop in an anterior to posterior direction (Wild 1999; Analía Púgener and Maglia 1997; Blanco and Sanchiz 2000; María Gabriela Perotti 2001; Pugener and Maglia 2009). If developmental timing predictably affects the evolutionary rates of the anuran skeleton, anterior vertebrae should be more evolutionarily constrained than posterior vertebrae. However, no studies to date have examined whether developmental timing affects vertebrae shape evolution.

Here, we provide the first macroevolutionary examination of anuran vertebrae shape to better understand the intrinsic and extrinsic factors influencing anuran presacral vertebrae shape evolution. We used microcomputed tomography (microCT) scans of 209 anuran species, three-dimensional geometric morphometrics, and phylogenetic comparative methods to (1) test for variation in phylogenetic modularity and evolutionary rates among vertebrae, (2) test for vertebrae shape and evolutionary rate variation associated with adult body size, adult microhabitat, and larval habitat, and (3) examine the relationship between relative

vertebrae developmental timing and vertebrae evolutionary rates. In examining the evolution of anuran vertebrae, we provide a unique comparison to vertebral evolution in other tetrapods and a jumping-off point for comparative evolutionary and developmental studies on anuran vertebrae.

Methods And Materials

DATA COLLECTION AND microCT SCANNING OF MUSEUM SPECIMENS

Of the 209 specimens used in this study (each belonging to a unique species), 203 specimens were microCT scanned for this study and an additional six specimen scans were downloaded from Morphosource (http://www.morphosource.org). Our sampling includes at least one species from 47 of the extant 54 anuran families. All specimens used in this study are museum specimens from the National Museum of Natural History ($n = 123$), Museum of Vertebrate Zoology ($n = 80$), California Academy of Sciences ($n = 2$), Centre for Ecological Sciences ($n = 1$), Museum of Comparative Zoology ($n = 1$), University of Kansas Biodiversity Institute ($n = 1$), and University of Florida ($n = 1$) herpetology collections. We microCT scanned the 203 specimens loaned from the National Museum of Natural History and the Museum of Vertebrate Zoology using a Phoenix vjtomejx M (GE Measurement & Control Solutions, Boston, MA), at the University of Florida's Nanoscale Research Facility. We performed all scans with a 180-kV X-ray tube containing a diamond-tungsten target, with the voltage, current, and detector capture time adjusted for each scan to maximize absorption range. We reconstructed all scans on GE's datosjx software version 2.3 and segmented all skeletons using VG StudioMax (Volume Graphics, Heidelberg, Germany). All scans are available for download on Morphosource (http://www.morphosource.org, project number P967) and information on all specimens used in this study (including those downloaded from morphosource.org) can be found in Table S1.

We measured snout-vent length (SVL) of all loaned specimens to the nearest 10th mm using a digital caliper (31-415-3, Swiss Precision Instruments, Inc., Garden Grove, CA) and measured SVL of all skeleton models downloaded from Morphosource in Meshlab (Cignoni et al. 2008). We classified larval habitat as direct developer, lotic tadpole, or lentic tadpole, for 176 species from 138 primary literature sources (see Table S1) as well as secondary references and databases, AmphibiaWeb (amphibiaweb.org), IUCN (IUCN 2021), and the AmphiBio database (Oliveira et al. 2017). We classified adult microhabitat for 207 species using data previously collated (Buttimer et al. 2020; Stepanova and Womack 2020) from primary (Andreone and Luiselli 2003; McCranie and Castañeda 2005; Brito et al. 2012; Matojo 2015) and secondary references (IUCN 2021; Moen et al. 2016; Moen and Wiens 2017; AmphibiaWeb [amphibiaweb.org]). We used seven of the eight microhabitat categories defined by Moen and Wiens (Moen and Wiens 2017): (1) aquatic—usually in water, (2) arboreal—typically on aboveground vegetation, (3) burrowing—nonbreeding season spent underground or in burrows they dug, (4) semi-aquatic—partially aquatic and partially terrestrial, (5) semi-arboreal—partially arboreal and partially terrestrial, (6) semi burrowing—partially burrowing and partially terrestrial, (7) terrestrial—found on the ground, under rocks, or in leaf litter, and (8) torrential—found in high-gradient, fast-flowing streams. We did not include any semi-burrowing species in this study. All associated data and references are in Table S1.

LANDMARKING VERTEBRAE

After obtaining skeleton meshes of all scans, seven landmarks were placed on each presacral vertebrae of each specimen using the digit.fixed function in the R package *geomorph* version 4.0.0 (Adams et al. 2021; Baken et al. 2021). All downstream analyses were likewise performed in R version 4.1.0 (R Core Team 2021). The seven landmarks corresponded to homologous and repeatable points that defined the outer borders of the vertebrae (Fig. 1). Six landmarks were in positions on the dorsal face of the vertebral column. Two of these were placed on either the right or left caudal tip. Another two landmarks were placed on the transverse process tips (one on the left and one on the right). When transverse processes widened toward their terminus rather than coming to a point, landmarks were placed at the center of the tip. Two additional landmarks were placed along each vertebra's central axis: one at the cervical edge between the transverse processes and another at the caudal edge between the caudal tips. The seventh landmark was also placed on the central axis at the cervical edge but on the ventral face of the column rather than the dorsal face. We assessed landmark placement reliability by having at least two separate researchers landmark 80 of our 209 specimens. We performed a generalized Procrustes analysis (GPA) on each vertebra that had multiple landmarkers, performed a principal components analysis (PCA) on the aligned landmarks for each vertebra, and compared within-specimen variation in the PCA results. To quantify variation among landmarkers, we added the standard errors of the first four PCA axes for each specimen and compared the sum of these standard errors among specimens, looking for outlier specimens with high standard errors. We also visually inspected the proximity of landmarked vertebrae in the first four principal components to verify inconsistencies among landmarkers. This sum-of-standard-errors approach provided a quality control step that caught large landmarking differences among researchers, including landmarking errors. We found the landmarks in this study were reliably placed across all anuran families and provided novel information, because we could find

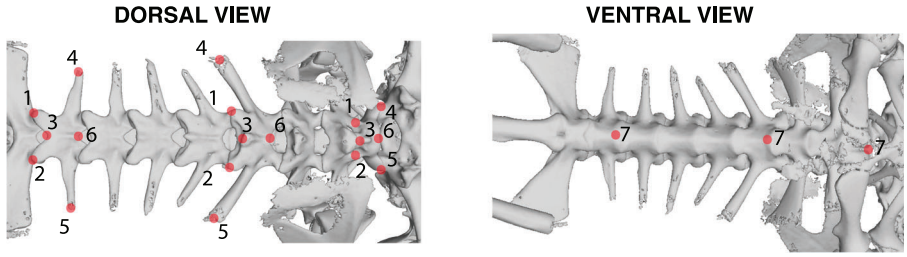

Figure 1. Example landmarks on the first (cervical), third, and eighth presacral vertebrae of a representative micoCT scan. These same seven landmarks were placed on all presacral vertebrae of each specimen and are described in the methods text.

no other study that analyzed vertebrae in three dimensions at the macroevolutionary scale.

COMPARING SHAPE EVOLUTION AMONG VERTEBRAE

To compare shape variation among vertebrae, we first performed a GPA on each vertebra (209 species, 1650 total vertebrae) to translate all vertebrae to the origin, scale them to unit-centroid size, and rotate them (using a least-squares criterion) until the landmarks were optimally aligned (Gower 1975; Rohlf and Slice 1990) using the gpagen function in the R package *geomorph* version 4.0 (Collyer and Adams 2018, 2021; Adams et al. 2021; Baken et al. 2021). We then ran PCA to visually compare shape variation among vertebrae. To determine whether vertebrae shape was associated with a vertebrae's position along the vertebral column, we ran a multivariate analysis of variance (MANOVA) using the procD.lm function in the R package *geomorph* version 4.0 (Collyer and Adams 2018, 2021; Adams et al. 2021; Baken et al. 2021) with the all aligned vertebrae for each specimen as the dependent variable and vertebral position (first vertebrae, second vertebrae, etc.) as the independent variable. However, we did not include the ninth presacral vertebrae because only three species (*Ascaphus montanus*, *Dendrobates auratus*, and *Leiopelma hamiltoni*) had nine presacral vertebrae. We then performed pairwise post hoc analyses to compare vertebrae shape among individual vertebrae.

COMPARING PHYLOGENETIC MODULARITY AND EVOLUTIONARY RATES AMONG VERTEBRAE

To determine which vertebrae were evolving at differing rates or in coordinated ways, we determined the evolutionary rate and degree of phylogenetic modularity among vertebrae. We only included the first seven vertebrae for these analyses because not all 209 specimens had an eighth vertebrae. We also excluded two species (*Myobatrachus gouldii* and *Craugastor laticeps*) from our study that had only six presacral vertebrae. We aligned the landmarks of each of the first seven vertebrae using a GPA (as above) and then combined these seven vertebrae via the combine.subsets function in the R package *geomorph* version 4.0 (Collyer and Adams 2018, 2021; Adams et al. 2021; Baken et al. 2021), which merges these separate vertebra landmark sets into a single morphological dataset. We did not perform a second GPA during implementation of combine.subset function (option GPA = FALSE), so that vertebrae were equally scaled in our analysis and to avoid introducing covariances that can mislead modularity analyses when modules are subsets of a common Procrustes superimposition (Cardini 2019). We then pruned an already published amphibian phylogenetic tree (Pyron 2014) to match the species in this study. We then calculated and compared net rates of morphological evolution among vertebrae, under a Brownian motion model of evolution (as in Denton and Adams 2015) using the compare.multi.evol.rates function in the R package *geomorph* version 4.0 (Collyer and Adams 2018, 2021; Adams et al. 2021; Baken et al. 2021). Additionally, we used the phylo.modularity function to quantify the degree of phylogenetic modularity in each vertebra by the pairwise covariance ratio (CR: see Adams 2016), under a Brownian motion model of evolution. A significant modular signal is found when the observed covariance ratio coefficient between two vertebrae is small compared to a distribution of values obtained by randomly assigning landmarks into subsets. The pairwise matrix of vertebrae modularity was plotted using the R package *ggplot2* version 3.3.3 (Wickham 2016).

TESTING THE ASSOCIATION BETWEEN INDIVIDUAL VERTEBRA SHAPE AND PHYLOGENY, BODY SIZE, ADULT MICROHABITAT, AND LARVAL HABITAT

We first examined vertebrae individually to see whether certain vertebrae (e.g., the cervical vertebrae) show stronger associations between vertebrae shape and body size, adult microhabitat, or larval habitat than other vertebrae. To test whether individual vertebra shape was associated with body size, adult microhabitat, or larval habitat, we performed MANOVAs that accounted for phylogenetic relationships among species using the procD.pgls function in the R package *geomorph* version 4.0 (Collyer and Adams 2018, 2021; Adams et al. 2021; Baken et al. 2021). As above, we first performed a GPA on each vertebral position.

We then estimated the phylogenetic signal of vertebrae shape evolution at each vertebral position to understand if phylogeny influences variation in vertebrae shape and if the strength of phylogenetic influence varies among individual vertebrae. We estimated phylogenetic signal with the physignal function in the R package geomorph version 4.0.0 (Adams et al. 2021; Baken et al. 2021), which estimates the multivariate version of the *K*-statistic (Kmult [Adams 2014]). For each vertebral position, we then ran three separate MANOVAs. All MANOVAs had vertebrae shape data from a single vertebral position as the dependent variable and the log of the specimen's SVL as a covariate. Additionally, one MANOVA had species' adult microhabitat as the independent variable to test whether adult microhabitat affected vertebrae shape. The second MANOVA included the interaction between adult microhabitat and the log of the specimen's SVL to test whether adult microhabitat affected the relationship between body size and vertebrae shape (allometry). The third MANOVA had larval habitat (instead of adult microhabitat) as an independent variable to test whether larval habitat affected vertebrae shape. We subsequently performed post hoc pairwise comparisons among adult microhabitat and larval habitat for each vertebral position.

Results of the first MANOVA that had species' adult microhabitat as the dependent variable and SVL as a covariate were plotted using the R package *ggplot2* version 3.3.3 (Wickham 2016). Results of the second MANOVA that included the interaction between adult microhabitat and the log of the specimen's SVL were plotted using the function plot.allometry in the R package *geomorph* version 4.0 (Collyer and Adams 2018, 2021; Adams et al. 2021; Baken et al. 2021). Pairwise post hoc comparisons for both MANOVAs were plotted using *ggplot2* version 3.3.3 (Wickham 2016).

TESTING THE ASSOCIATION BETWEEN THE COMBINED SHAPE OF THE FIRST SEVEN PRESACRAL VERTEBRAE AND BODY SIZE, ADULT MICROHABITAT, AND LARVAL HABITAT

To test whether the combined shape of the first seven presacral vertebrae, which contains more shape variation among species than an individual vertebra, was associated with body size, adult microhabitat, or larval habitat, we performed MANOVAs that accounted for phylogenetic relationships among species. As with our evolutionary rates and phylogenetic modularity analyses, we only included the first seven vertebrae for these analyses. But unlike our evolutionary rates and phylogenetic modularity analyses, we combined these seven vertebrae via the combine.subsets during which we performed a second GPA (using option GPA = TRUE), which scaled bones to their unit-centroid size and resulted in correct vertebrae proportions. We then used the procD.pgls function to run the same three MANOVAs and post hoc pairwise comparisons that we ran with each individual vertebrae, but we used the combined first seven vertebrae shape data as the dependent variable.

Results

SHAPE VARIATION AND MODULARITY ALONG THE ANURAN VERTEBRAL COLUMN

When the shapes of all the vertebrae of each specimen are analyzed, we found a significant association of vertebrae shape with its position along the vertebral column ($F_{7,1642} = 462.78$, $R^2 = 0.66$, $P < 0.001$). Post hoc pairwise comparisons among vertebrae showed that each vertebrae had a distinct average shape from every other vertebra in the column. A PCA revealed that vertebrae 1, 2, and 3 are especially distinct and more like one another than to vertebrae 4 through 8, which clustered more closely together along the first principal component (Fig. 2a). In addition, we found phylogenetic modularity varies among vertebrae (CR = 0.67, effect size = –5.00, $P < 0.001$). We saw an overall pattern of increased phylogenetic modularity (increased shape correlation within vertebrae compared to between vertebrae) as we moved posteriorly, with lower modularity in the first (cervical) vertebrae and second presacral vertebrae and very high modularity among the fifth, sixth, and seventh vertebrae (Fig. 2b).

EVOLUTION RATES AND PHYLOGENETIC SIGNAL ALONG THE ANURAN VERTEBRAL COLUMN

We found variation among vertebrae in the evolutionary rate and phylogenetic signal of vertebra shape. Evolutionary rates varied among vertebrae (effect size = 9.42, $P < 0.001$), with the cervical vertebrae having the highest evolutionary rate and the second vertebrae having the lowest evolutionary rate (Fig. 3a). A stepwise increase in evolutionary rates was found in vertebrae 2–7, except for no difference in evolutionary rate between vertebrae 3 and 4 (Fig. 3a). Meanwhile, phylogenetic signal was similar among vertebrae 1 through four ($K = 0.33$–0.42) and then sharply increased for vertebrae 5–7 ($K = 0.78$–0.85; Fig. 3b; Table 1). We found a slight decrease in phylogenetic signal in vertebrae 8 ($K = 0.64$, Fig. 3b) where sample size is lower, due to fewer species having eight vertebrae (Table 1).

EVOLUTION OF INDIVIDUAL VERTEBRAE IN RELATION TO BODY SIZE, ADULT MICROHABITAT, AND LARVAL HABITAT

We found variation among vertebrae in their associations with body size, adult microhabitat, and larval habitat (Fig. 3c). Each vertebra shape had a significant relationship with SVL and adult microhabitat (Table 1). SVL explained the largest amount of individual vertebrae shape variation, with vertebra one, two, and eight having lower associations with SVL (8%–10% *R*-squared;

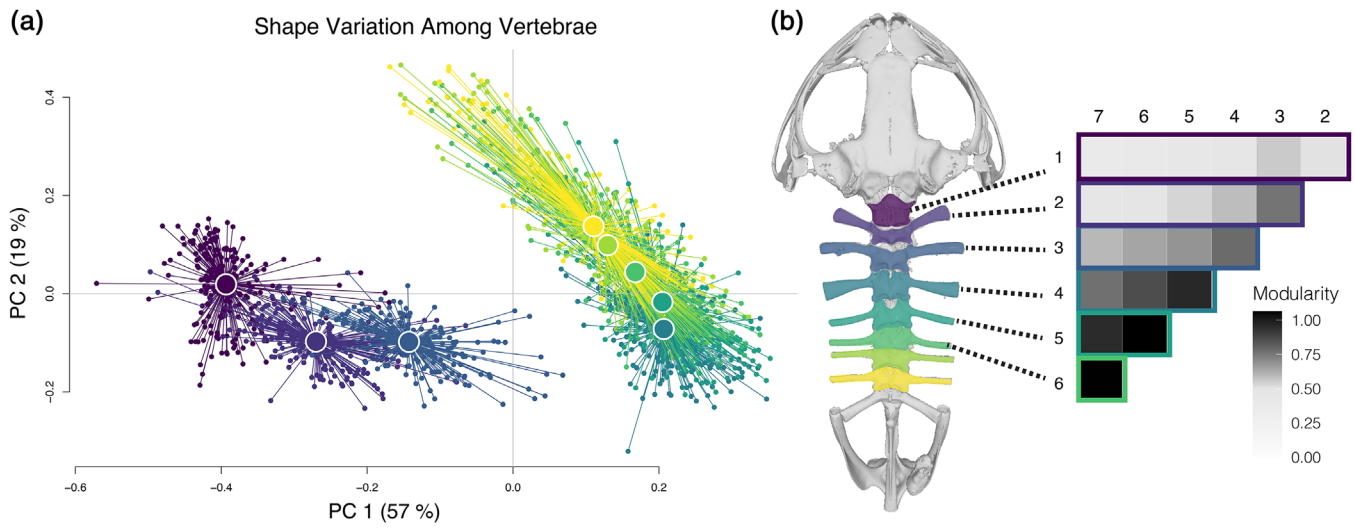

Figure 2. A principal component analysis (a) and correlation plot of pairwise modularity estimates (b) for presacral vertebrae shape. Colors indicate the position of the vertebrae along the column, with the first (cervical) presacral vertebrae in purple and the eighth presacral vertebrae in yellow. Panel (b) grayscale shows modularity as a pairwise covariance ratio coefficient, in which a more modular signal (darker) indicates the observed covariance ratio coefficient between two vertebrae is small compared to a distribution of values obtained by randomly assigning landmarks into subsets.

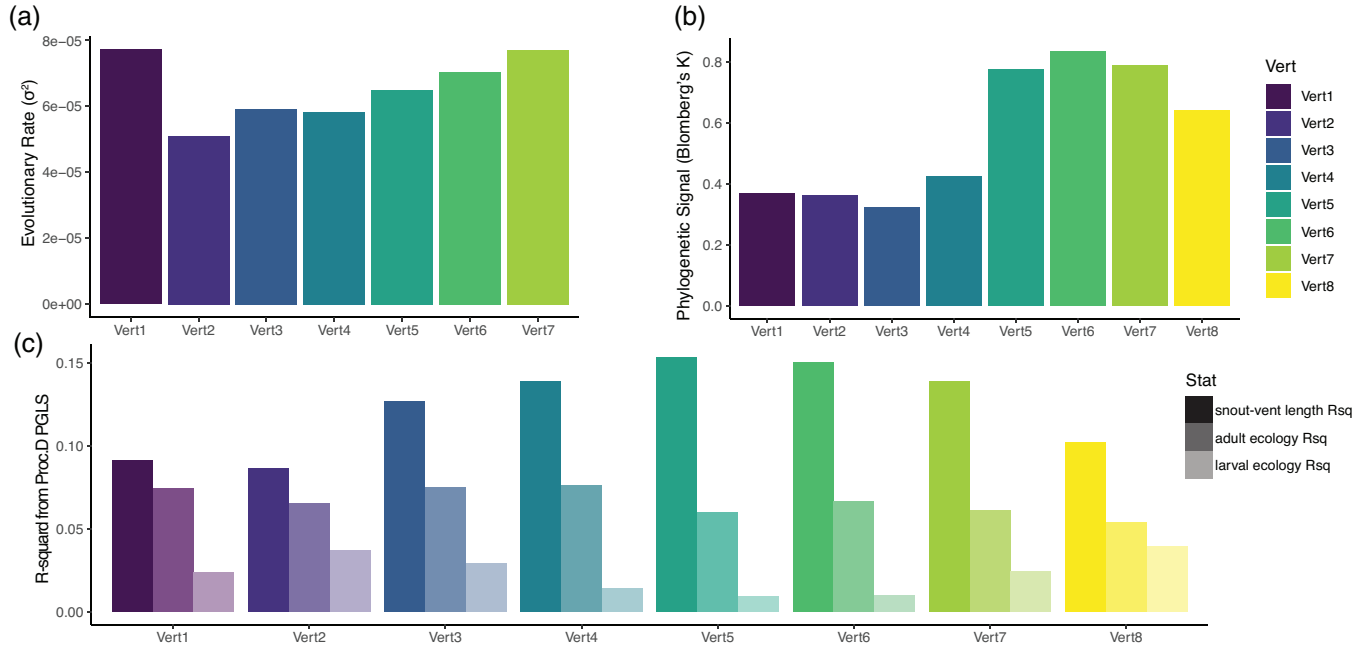

Figure 3. Bar graphs showing variation among individual vertebrae in evolutionary rates of vertebrae shape (a), phylogenetic signal of vertebrae shape (b), and the relationship between vertebrae shape and snout-vent length, adult microhabitat, and larval habitat (c). Colors indicate the position of the vertebrae along the column, with the first (cervical) presacral vertebrae in purple and the eighth presacral vertebrae in yellow.

Table 1; Fig. 3c) and vertebrae 3–7 having higher associations with SVL (13%–16% *R*-squared; Table 1; Fig. 3c). Adult microhabitat was significantly associated with individual vertebrae shape and explained a consistent amount of variation in all vertebrae (5%–8% *R*-squared; Table 1; Fig. 3c). We found a significant association between individual vertebrae shape and larval habitat (lotic tadpoles, lentic tadpoles, or direct development) for all vertebrae except vertebrae 4–6. However, the shape variation explained by larval habitat was less than 4% (Table 1; Fig. 3c) in all cases.

Table 1. Estimates of phylogenetic signal and results from phylogenetic MANOVAs that test for associations between vertebrae shape and body size, adult microhabitat, and larval ecology.

	Phylogenetic Signal	Body Size Log(SVL)	Adult Microhabitat	Larval Habitat
First vertebrae	$K = 0.37$	$F_{1,199} = 22.19, Z = 6.74$	$F_{6,199} = 3.01, Z = 3.46$	$F_{2,172} = 2.70, Z = 2.76$
	$P < 0.001$***	$R^2 = 0.09$	$R^2 = 0.08$	$R^2 = 0.03$
	$N = 206$	$P < 0.001$***	$P < 0.001$***	$P = 0.005$**
Second vertebrae	$K = 0.37$	$F_{1,199} = 19.87, Z = 5.94$	$F_{6,199} = 2.71, Z = 3.58$	$F_{2,172} = 3.30, Z = 2.90$
	$P < 0.001$***	$R^2 = 0.08$	$R^2 = 0.07$	$R^2 = 0.03$
	$N = 206$	$P < 0.001$***	$P < 0.001$***	$P < 0.003$***
Third vertebrae	$K = 0.33$	$F_{1,199} = 31.34, Z = 8.12$	$F_{6,199} = 3.31, Z = 4.15$	$F_{2,172} = 2.83, Z = 2.83$
	$P < 0.001$***	$R^2 = 0.13$	$R^2 = 0.08$	$R^2 = 0.03$
	$N = 206$	$P < 0.001$***	$P < 0.001$***	$P < 0.003$***
Fourth vertebrae	$K = 0.42$	$F_{1,199} = 36.63, Z = 7.13$	$F_{6,199} = 3.13, Z = 4.39$	$F_{2,172} = 1.80, Z = 1.63$
	$P < 0.001$***	$R^2 = 0.14$	$R^2 = 0.07$	$R^2 = 0.02$
	$N = 206$	$P < 0.001$***	$P < 0.001$***	$P = 0.05$
Fifth vertebrae	$K = 0.78$	$F_{1,199} = 40.61, Z = 6.45$	$F_{6,199} = 2.40, Z = 3.41$	$F_{2,172} = 1.24, Z = 0.72$
	$P < 0.001$***	$R^2 = 0.16$	$R^2 = 0.06$	$R^2 = 0.01$
	$N = 206$	$P < 0.001$***	$P < 0.001$***	$P = 0.240$
Sixth vertebrae	$K = 0.84$	$F_{1,199} = 39.46, Z = 5.70$	$F_{6,199} = 2.67, Z = 3.53$	$F_{2,172} = 1.36, Z = 0.90$
	$P < 0.001$***	$R^2 = 0.16$	$R^2 = 0.06$	$R^2 = 0.01$
	$N = 206$	$P < 0.001$***	$P < 0.001$***	$P = 0.187$
Seventh vertebrae	$K = 0.79$	$F_{1,198} = 33.84, Z = 5.47$	$F_{6,198} = 2.53, Z = 3.16$	$F_{2,171} = 2.33, Z = 1.94$
	$P < 0.001$***	$R^2 = 0.14$	$R^2 = 0.06$	$R^2 = 0.02$
	$N = 205$	$P < 0.001$***	$P < 0.001$***	$P = 0.027$*
Eighth vertebrae	$K = 0.64$	$F_{1,178} = 21.19$	$F_{6,178} = 1.87, Z = 2.24$	$F_{2,152} = 3.54, Z = 2.83$
	$P < 0.001$***	$Z = 5.02$	$R^2 = 0.05$	$R^2 = 0.04$
	$N = 184$	$R^2 = 0.10$	$P = 0.012$**	$P = 0.002$**
		$P < 0.001$***		

*$P < 0.05$; **$P < 0.01$; ***$P < 0.001$.

Although the amount of variation explained by adult microhabitat was similar among vertebrae, the pairwise differences between microhabitats varied by vertebrae (Fig. 4). Arboreal species consistently differed in vertebrae 1 shape compared to burrowing, aquatic, and terrestrial species (Fig. 4i), with relatively wide and less rostrocaudally lengthened cervical vertebrae (Fig. 4a). Additionally, arboreal and burrowing species consistently differed in vertebrae 2–7 shape (Fig. 4i) with burrowing species having shorter relative transverse processes (depicted by differences along PC1 in Fig. 4b–g). Arboreal species also consistently differed from semi-aquatic species in vertebrae 2–6 (Fig. 4b–f,i). For particular vertebrae, burrowing and arboreal species both showed differences in vertebrae shape compared to terrestrial and semi-arboreal species and arboreal species showed some additional individual vertebrae shape differences compared to aquatic species (Fig. 4i).

The relationship between SVL and vertebrae shape (allometry) differed among adult microhabitats for vertebrae 2–8 (Fig. 5a–h); however pairwise differences between microhabitats varied by vertebrae (Fig. 5i). Burrowing and aquatic species had consistently different allometries than arboreal, semi-aquatic, semi-arboreal, and terrestrial species in at least one vertebra. Burrowing species were most differentiated in allometry in vertebrae 3–8, seemingly due to shorter and more posteriorly oriented transverse processes, especially when compared to arboreal and semi-aquatic species (Fig. 5c–i). Contrastingly, aquatic species were most allometrically different in vertebra 2, and occasionally vertebrae 3 or 4, seemingly due to lengthened transverse processes (Fig. 5b,c,i).

EVOLUTION OF VERTEBRAL COLUMN IN RELATION TO PHYLOGENY, SVL, ADULT MICROHABITAT, AND LARVAL HABITAT

When the first seven presacral vertebrae were analyzed in combination, we found similar results as those for individual vertebra shape. We found vertebral column shape had significant phylogenetic signal ($K = 0.58$, $P < 0.001$) and that SVL explained the largest amount of vertebral column shape variation ($F_{1,198} = 31.25$, $R^2 = 0.13$, $P < 0.001$), followed by adult microhabitat ($F_{6,198} = 2.78$, $R^2 = 0.07$, $P < 0.001$), and

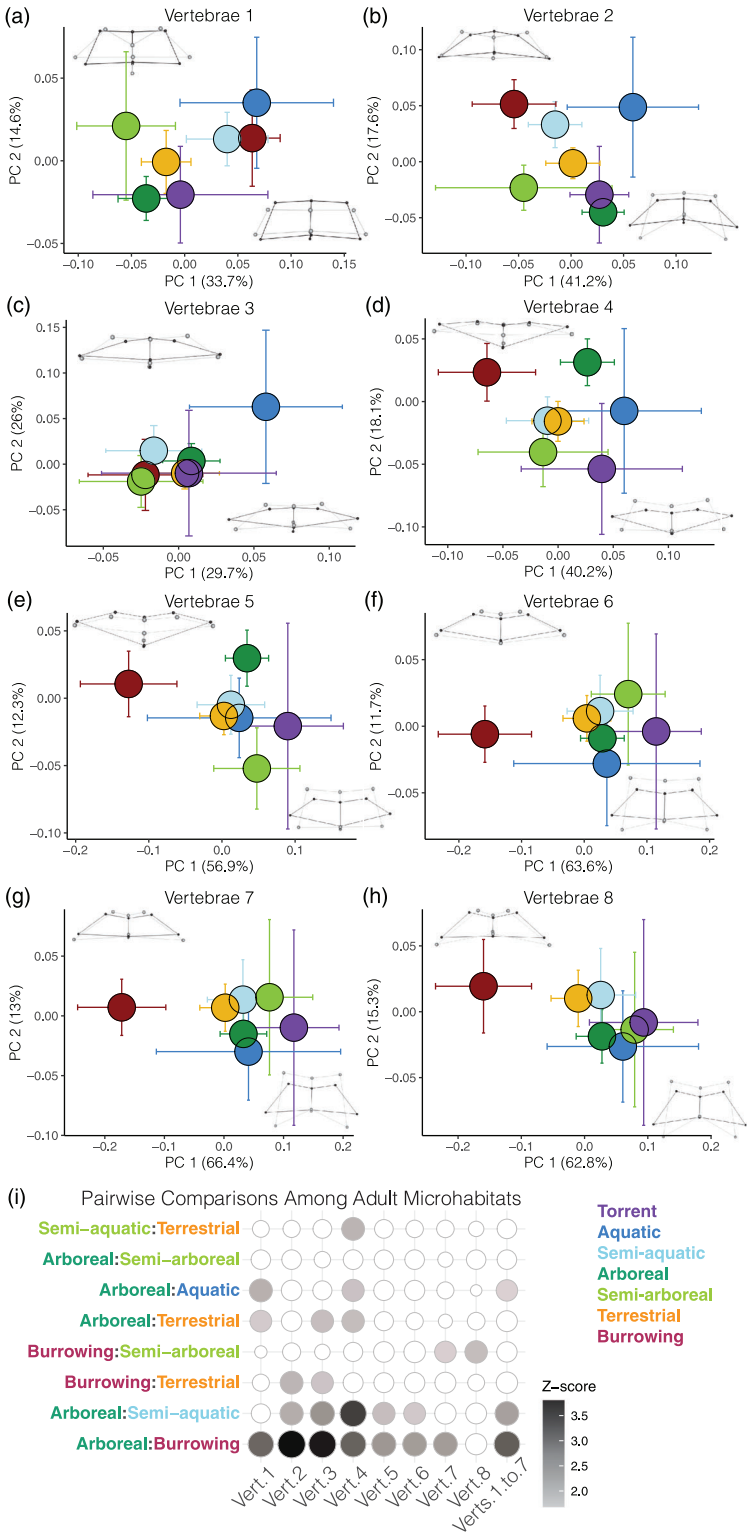

Figure 4. Principal component analysis and post hoc pairwise comparisons of individual presacral vertebrae shape variation among species that occupy different microhabitats. (a–h) Each PCA plot shows the centroids for each microhabitat with 95% confidence intervals represented with error bars. In each plot, wire frame outlines, generated with the shape.predictor function, display the predicted vertebra shape change between the minimum (gray) and maximum (black) PC1 (bottom right) and PC2 (top left) with a 0.5 magnification. (i) Post hoc pairwise comparisons of vertebrae shape between adult microhabitats from MANOVAs accounting for body size and phylogenetic relationships. Only microhabitat comparisons with at least one significant difference are shown. The *Z*-score of each pairwise comparison is indicated by the size of the circle (smaller = closer to zero) and filled circles indicate statistically significant differences. Scale colors used from the Wes Anderson color palette "Isle of Dogs 1" (Ram and Wickham 2018).

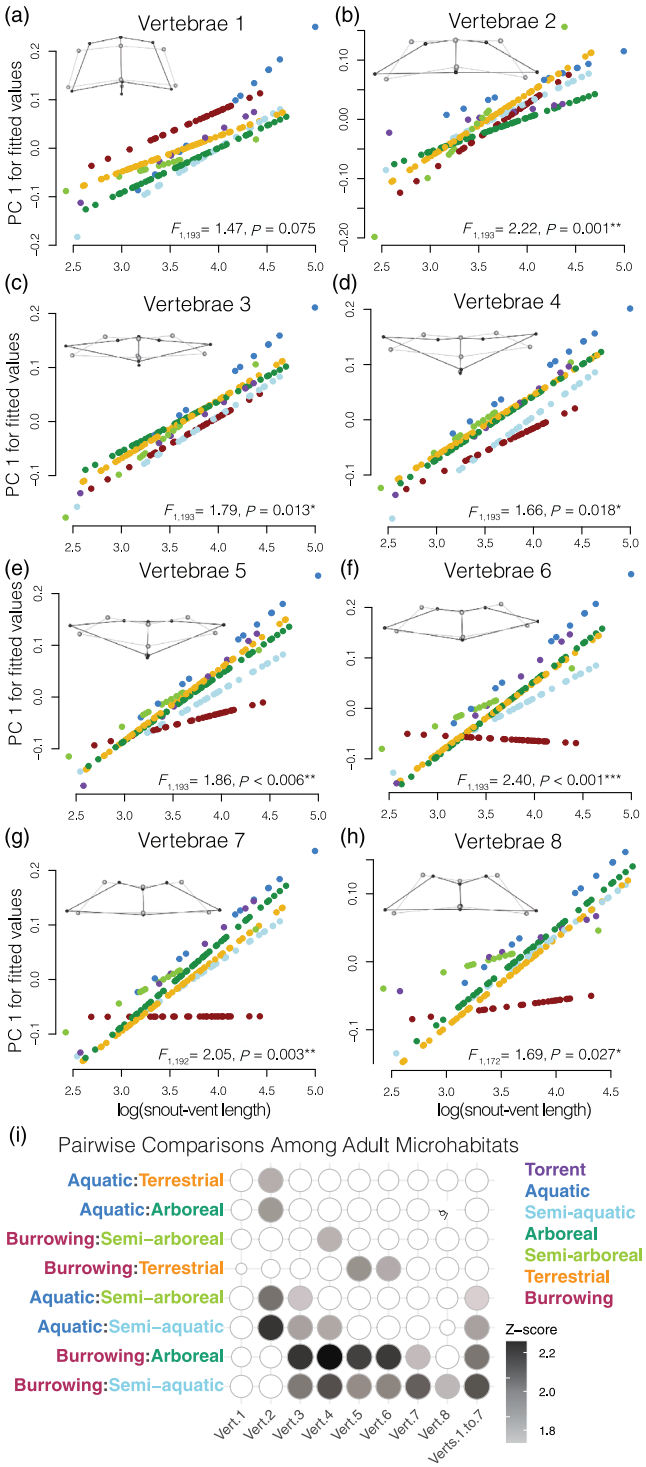

Figure 5. Relationship between individual vertebrae shape and body size (allometry) post hoc pairwise comparisons of individual vertebrae allometry among adult microhabitats. (a–h) Each scatterplot shows the relationship between log snout-vent length and the first principal component of the "predicted" values versus size from a procD.lm fit for each microhabitat. In each plot, wire frame outlines, generated with the shape.predictor function, display the predicted vertebra shape change between the minimum (gray) and maximum (black) snout vent lengths with a 1.0 magnification. *F*-statistics and *P* values are given for the interaction between snout-vent length and adult microhabitat from phylogenetic MANOVAs. (i) Post hoc pairwise comparisons of the relationship (slope) between snout-vent length and vertebrae shape between adult microhabitats from phylogenetic MANOVAs accounting for phylogenetic relationships. Only microhabitat comparisons with at least one significant difference are shown. The *Z*-score of each pairwise comparison is indicated by the size of the circle (smaller = closer to zero) and filled circles indicate statistically significant differences. Scale colors used from the Wes Anderson color palette "Isle of Dogs 1" (Ram and Wickham 2018).

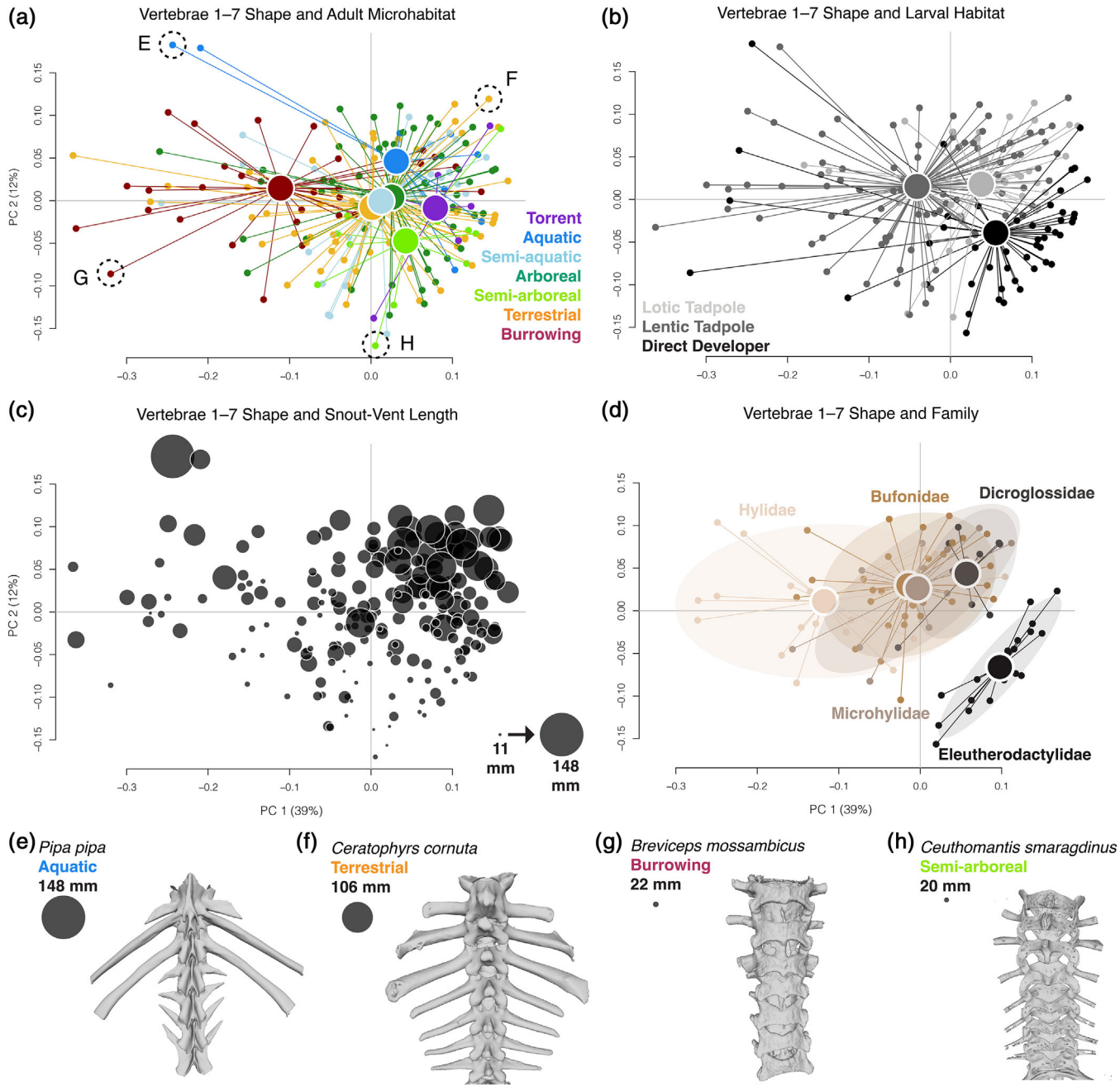

Figure 6. Principal component analyses of the combined shape of the first seven presacral vertebrae displaying the relationship between vertebral column shape and adult microhabitat (a), larval habitat (b), snout-vent length (c), and phylogeny (d). (a) Adult microhabitat is indicated by color and centroids for each microhabitat are connected to the individual species shape data. (b) Larval habitat is indicated by color and centroids for each larval habitat are connected to the individual species shape data. (c) Snout-vent length of each specimen is indicated by the size of the dot. (d) Family is indicated by color and centroids for each family are connected to the individual species shape data. Only the five families with 10 or more species in our dataset are shown. Family colors are from the Wes Anderson color palette "Isle of Dogs 2" (Ram and Wickham 2018). (e–h) Example vertebrae from four species highlighted with dotted circles in panel (a)

larval habitat explained very little vertebral column shape variation ($F_{2,171} = 2.19$, $R^2 = 0.02$, $P = 0.004$). Burrowing, aquatic, and semi-aquatic species all had a significantly different average vertebral column shape from arboreal species (Figs. 4i, 6a). We found no overall difference in vertebral column shape evolutionary rates among species with differing adult microhabitats (effect size = –0.12, $P = 0.542$) or larval habitat (effect size = –0.06, $P = 0.518$). However, we found differences in vertebral column shape allometry among adult microhabitats ($F_{6,192} = 1.92$, $R^2 = 0.05$, $P < 0.001$). Burrowing species had

distinct vertebral column allometries from semi-aquatic and arboreal species (Fig. 5i). Semi-aquatic species also differed in vertebral column allometry from aquatic species (Fig. 5i).

Discussion

In this first three-dimensional macroevolutionary analysis of frog presacral vertebrae shape, we identified distinct evolutionary patterns between the cervical vertebra and the trunk vertebrae, as well as variation in evolutionary patterns among trunk vertebrae. We also found that vertebrae shape is more associated with differences in body size than differences in adult microhabitat or larval habitat among species. Although we found no differences in evolutionary rates of vertebrae shape among adult or larval ecologies, we did find variation in evolutionary rates of vertebrae shape related to developmental timing, reinforcing the hypothesis that later developing traits are more evolutionarily variable.

VARIATION IN SHAPE AMONG PRESACRAL ANURAN VERTEBRAE

Our data reveal region-specific patterns of trunk vertebrae evolution within Anura's shortened vertebral column. We show that, like many other tetrapod clades, anuran presacral vertebrae have differing evolutionary rates and phylogenetic modularity along the vertebral column. We found the cervical vertebra (the most rostral presacral vertebra) had a distinct shape and high evolutionary rate when compared with other presacral vertebrae. The high evolutionary rate of the cervical vertebrae in Anura counters the conserved shape of cervical vertebrae in other tetrapods, such as carnivorans (Randau and Goswami 2017, 2018). Although we found no differences in evolutionary rates among microhabitats, the increased evolutionary rate of the cervical vertebrae could be related to selection pressures for cranial stabilization during more specific locomotor modes, such as head-first burrowing, that we did not examine in this study. Furthermore, the similarity in shape of the fourth through eighth presacral vertebrae combined with the higher modularity among these vertebrae suggests these posterior presacral vertebrae may be evolving as a distinct module from second and third presacral vertebrae. Unlike the lumbar vertebrae of felids that seem to form a functional module (Randau et al. 2016; Randau and Goswami 2017; Jones et al. 2018b), we lack evidence that ecological selection pressures had a substantial influence on the shape evolution of anuran posterior presacral vertebrae. Instead, we found anuran posterior presacral vertebrae have high phylogenetic signals, indicating they are evolving closer to the expectations of Brownian motion than the cervical vertebrae and the first two trunk vertebrae. Thus, we hypothesize that shared genetic, developmental, or functional interactions associated with phylogeny are influencing the evolution of anuran posterior presacral vertebrae.

Serial homologous structures (like vertebrae) are initially formed by duplicated developmental programs (Hall 1995). Despite this initial integration from shared development, serially homologous structures often become more modular over evolutionary time, leading to modification, or even loss, of individual components (reviewed in Sadier et al. 2022). Anuran presacral vertebrae provide another example of serially homologous structures that have differentiated over millions of years, although the exact reasons for anuran presacral vertebrae differentiation remain unclear. By identifying large differences in presacral vertebrae evolution among individual vertebrae, as well as among anuran clades, our data provide a starting point for comparative research into the genetic and developmental underpinnings of anuran presacral vertebrae differentiation.

LIMITED EVIDENCE FOR SELECTION PRESSURES RELATED TO LARVAL AND ADULT ECOLOGY ON PRESACRAL VERTEBRAE SHAPE EVOLUTION

Adult microhabitat explains very little variation in presacral vertebrae shape and larval habitat explains even less, indicating that adult and larval ecologies do not impose strong selection pressures on presacral vertebrae shape. The low associations between presacral vertebrae shape and adult microhabitat are consistent with low association between anuran pelvic features and adult microhabitat, including the sacral vertebrae and urostyle (Buttimer et al. 2020). Furthermore, the consistently low association between vertebrae shape and adult and larval ecology indicates that, although presacral vertebrae show modularity, they lack evidence for functional regionalization. This contrasts the evidence for function-based modules in other tetrapod groups, such as mammals (Randau et al. 2016; Randau and Goswami 2017; Jones et al. 2018b) and ray-finned fishes (Maxwell et al. 2021). Our findings also contrast evidence for function-based evolution of other skeletal features, such as anuran limb bone shapes, in which adult microhabitat explains up to 17% of interspecific limb bone shape variation in the distal limb bones (Stepanova and Womack 2020).

However, the differentiation in vertebrae shape between burrowing and arboreal anurans, specifically differences in transverse processes, supports descriptive findings from previous comparative studies that showed burrowing, walking, and hopping anurans had distinct presacral vertebrae characteristics (Emerson 1982). Although Moen (2019) found no difference in jump velocity evolutionary optima among anuran microhabitats, burrowing species are more often classified as hoppers or walkers than jumpers (Buttimer et al. 2020). Thus, selection pressures related to shorter jump distance or stabilization of the trunk against forces generated during digging may explain the distinct evolution of vertebrae shape in burrowing species. Furthermore, the shorter transverse processes of burrowing anurans

mirror the shorter transverse processes that characterize burrowing mammals (Jones et al. 2018b); however, scansorial/climbing and burrowing mammals show similar vertebrae shapes (Jones et al. 2018b), which contrasts the vertebrae shape differentiation we found between arboreal and burrowing anurans.

An even smaller amount of presacral vertebrae shape variation is associated with larval habitat, suggesting that the presacral vertebrae do not play a significant role in selective pressures associated with microhabitat at this stage in anuran development. This supports previous work that suggested the tail is the structure most responsible for variation in tadpole locomotion (Hoff and Wassersug 2000; Azizi et al. 2007). An alternative explanation is that the categories of lentic and lotic lack the specificity necessary to characterize the variation that is present. For example, some species of tadpoles exhibit burrowing that has been noted to lead to morphological differences such as the presence of caudal vertebrae (Handrigan and Wassersug 2007). This type of behavior might lead to significant variation in the shape of presacral vertebrae too but could not have been captured by our categorizations. Finally, there is the possibility that metamorphosis obscures the variation that is present during this stage by acting as a distinct boundary between larval and adult morphologies. Even if variation did exist in vertebral shape among larval anurans based on the selective pressures of this stage, metamorphosis (and associated cartilage remodeling) might act as a filter that reshapes differences in response to new selective pressures, conserving a distinct adult form (Moran 1994).

THE RELATIONSHIP BETWEEN BODY SIZE AND VERTEBRAE SHAPE

Anuran body size has the largest association with each individual vertebra's shape as well as overall vertebral column shape. Significant vertebrae allometry (the relationship between size and shape) has also been found in studies of mammals (Jones 2015; Randau et al. 2016; Jones et al. 2018b; Marchesi et al. 2021) and crocodilians (Iijima and Kubo 2019). However, the specific changes in vertebrae shape associated with larger body size differ from patterns found in mammals, which have craniocaudally shorter and dorsoventrally taller vertebrae in larger species (Jones 2015). In contrast, anuran species with larger body sizes have either minimal change in craniocaudal length or craniocaudally lengthened vertebrae (especially vertebrae 1, 4m and 5) and a general trend of more anteriorly positioned transverse process tips. Furthermore, in mammals, studies have found allometric differences between aquatic and terrestrial species (Jones and Pierce 2016) as well as between terrestrial and scansorial species (Randau et al. 2017). However, in anurans we mainly found differences in vertebrae allometric scaling in burrowing species when compared to semi-aquatic and arboreal species in vertebrae 3–8. Notably, aquatic species were most allometrically differentiated from other microhabitats in vertebra 2, and occasionally vertebrae 3 of four, further distinguishing the evolutionary patterns of anterior trunk vertebrae from more posterior trunk vertebrae.

EVIDENCE THAT DEVELOPMENTAL TIMING AFFECTS PRESACRAL VERTEBRAE SHAPE EVOLUTION

We found an increase in vertebra evolutionary rate along the vertebral axis, apart from the high cervical vertebrae evolutionary rate (discussed above). In the trunk vertebrae, we see a correlation between evolutionary rate of vertebra shape and timing of ossification, except for the third and fourth presacral vertebrae. The similar evolutionary rates of presacral vertebrae 3 and 4 are likely linked with their similar expansions and contractions of transverse process lengths, which are exaggerated in pipid frogs and show distinct evolutionary patterns from more posterior presacral vertebrae (as displayed in Fig. 6e). This increase in the evolutionary rate of trunk vertebrae shape along the vertebral column also correlates with the initial clock and wavefront process that lays down the axial skeleton from anterior to posterior during somitogenesis (Pourquié 2003; Gomez et al. 2008; Pourquié 2011). Our finding mirrors a study in mammals that found an increase in evolutionary rate as you move posteriorly in the vertebral column (Jones et al. 2018b). And the combination of higher evolutionary rates and more phylogenetic modularity of later-developing anuran presacral vertebrae adds interesting evidence toward speculation made by Randau and Goswami (2017), which showed strong covariation between the most anterior and most posterior presacral vertebrae that ossified later than other vertebrae. Furthermore, correlations between developmental timing and evolutionary rate have been found for other anuran skeletal traits, suggesting that those skeletal features are less developmentally constrained than earlier developing bones. Anuran limb bones (Stepanova and Womack 2020) and skull bones (Bardua et al. 2021) that develop and ossify later in ontogeny show more evolutionary lability and late-forming bones, such as digits (Alberch and Gale 1985) and middle ear bones (Pereyra et al. 2016), show more frequent evolutionary losses.

Conclusions

Many studies have analyzed the Bauplan of anurans; however, until now Anura's unique vertebral column remained unexamined at the macroevolutionary scale. Using phylogenetic comparative methods to look across hundreds of species, we found variation in shape and evolutionary rates among anuran vertebrae, dispelling any notion that trunk vertebrae evolve uniformly. In general, we found little evidence for selection pressures related to adult or larval ecology affecting presacral vertebrae evolution, but we did

find body size was most highly associated with vertebrae shape across all presacral vertebrae. Finally, this study contributes to rapidly growing evidence that increased evolutionary rates in later developing structures may be a theme in the anuran skeleton. Follow-up studies examining ontogenetic changes in gene expression as vertebrae develop could determine whether later developing vertebrae show higher evolutionary rates because of increased variation in gene expression. And species with extreme vertebrae morphologies, such as *Pipa pipa* or *Nasikabatrachus sahyadrensis*, provide excellent candidates for understanding the genetic underpinnings of presacral vertebrae shape evolution.

AUTHOR CONTRIBUTIONS

KAA and DLD contributed to the data collection, data analysis, and writing and editing of this manuscript. CMC contributed to the data collection and editing of this manuscript. MCW contributed to the conception of the study, data analysis, and writing and editing of the manuscript.

ACKNOWLEDGMENTS

We would like to thank E. Stanley and D. Blackburn for their help with microCT scans and reconstructions. We would like to thank WoLab members, J. Phillips, G. Mount, and M. Albecker, for their helpful comments on this manuscript. We would also like to thank the Smithsonian National Museum of Natural History and the Museum of Vertebrate Zoology for allowing us access to specimens used in this study. We would specifically like to thank A. Wynn and C. Spencer for their help with the specimen loans. This study was funded by the U.S. National Science Foundation (PRFB-1611752) and a Peter Buck Postdoctoral Fellowship from the Smithsonian National Museum of Natural History.

DATA ARCHIVING

Specimen information and species data used in all analyses can be found in Table S1 and in Dryad (https://doi.org/10.5061/dryad.gqnk98srq). Landmark data used in analyses can be found in Dryad (https://doi.org/10.5061/dryad.gqnk98srq).

CONFLICT OF INTEREST

The authors declare no conflict of interest.

REFERENCES

Adams, D.C. (2014) A generalized K statistic for estimating phylogenetic signal from shape and other high-dimensional multivariate data. *Syst. Biol.*, 63, 685–697.

———. (2016) Evaluating modularity in morphometric data: challenges with the RV coefficient and a new test measure. *Methods Ecol. Evol.*, 7, 565–572.

Adams, D.C., Collyer, M.L., Kaliontzopoulou, A. & Balken, E.K. (2021) Geomorph: software for geometric morphometric analyses. Available via https://cran.r-project.org/package=geomorph.

Alberch, P. & Gale, E.A. . (1985) A developmental analysis of an evolutionary trend: digital reduction in amphibians. *Evolution*, 39, 8–23.

Analía Púgener, L. & Maglia, A.M. (1997) Osteology and skeletal development of *Discoglossus sardus* (Anura: Discoglossidae). *J. Morphol.*, 233, 267–286.

Andreone, F. & Luiselli, L.M. (2003) Conservation priorities and potential threats influencing the hyper-diverse amphibians of Madagascar. *Ital. J. Zool.*, 70, 53–63.

Asher, R.J., Lin, K.H., Kardjilov, N. & Hautier, L. (2011) Variability and constraint in the mammalian vertebral column. *J. Evol. Biol.*, 24, 1080–1090.

Azizi, E., Landberg, T. & Wassersug, R.J. (2007) Vertebral function during tadpole locomotion. *Zoology*, 110, 290–297.

Baez, A.M., Trueb, L. & Calvo, J.O. (2000) The earliest known pipoid frog from South America: a new genus from the middle Cretaceous of Argentina. *J. Vertebr. Paleontol.*, 20, 490–500.

Baken, E.K., Collyer, M.L., Kaliontzopoulou, A. & Adams, D.C. (2021) geomorph v4.0 and gmShiny: enhanced analytics and a new graphical interface for a comprehensive morphometric experience. *Methods Ecol. Evol.*, 12, 2355–2363.

Bardua, C., Fabre, A.-C., Clavel, J., Bon, M., Das, K., Stanley, E.L., Blackburn, D.C. & Goswami, A. (2021) Size, microhabitat, and loss of larval feeding drive cranial diversification in frogs. *Nat. Commun.*, 12, 2503.

Bergmann, P.J. & Irschick, D.J. (2012) Vertebral evolution and the diversification of squamate reptiles. *Evolution*, 66, 1044–1058.

Blanco, M.J. & Sanchiz, B. (2000) Evolutionary mechanisms of rib loss in anurans: a comparative developmental approach. *J. Morphol.*, 244, 57–67.

Bonett, R.M. & Blair, A.L. (2017) Evidence for complex life cycle constraints on salamander body form diversification. *Proc. Natl. Acad. Sci. USA*, 114, 9936–9941.

Brito, L., Aguiar, F. & Cascon, P. (2012) Diet composition and activity patterns of *Odontophrynus carvalhoi* Savage and Cei, 1965 (Anura, Cycloramphidae) from a humid tropical rainforest in northeastern Brazil. *South Am. J. Herpetol.*, 7, 55–61.

Buttimer, S.M., Stepanova, N. & Womack, M.C. (2020) Evolution of the unique anuran pelvic and hind limb skeleton in relation to microhabitat, locomotor mode, and jump performance. *Integr. Comp. Biol.*, 60, 1330–1345.

Cannatella, D.C. & Trueb, L. (1988a) Evolution of pipoid frogs: intergeneric relationships of the aquatic frog family Pipidae (Anura). *Zool. J. Linn. Soc.*, 94, 1–38.

———. (1988b) Evolution of pipoid frogs: morphology and phylogenetic relationships of *Pseudhymenochirus*. *J. Herpetol.*, 22, 439–456.

Cardini, A. (2019) Integration and modularity in Procrustes shape data: is there a risk of spurious results? *Evol. Biol.*, 46, 90–105.

Cignoni, P., Callieri, M., Corsini, M., Dellepiane, M., Ganovelli, F. & Ranzuglia, G. (2008) MeshLab: an open-source mesh processing tool. Pp. 129–136 *in* Sixth Eurographics Italian Chapter Conference.

Collyer, M.L. & Adams, D.C. (2018) RRPP: an r package for fitting linear models to high-dimensional data using residual randomization. *Methods Ecol. Evol.*, 9, 1772–1779.

———. (2021) RRPP: linear model evaluation with randomized residuals in a permutation procedure. R package.

Denton, J.S.S. & Adams, D.C. (2015) A new phylogenetic test for comparing multiple high-dimensional evolutionary rates suggests interplay of evolutionary rates and modularity in lanternfishes (Myctophiformes; Myctophidae). *Evolution*, 69, 2425–2440.

Emerson, S.B. (1982) Frog postcranial morphology: identification of a functional complex. *Copeia*, 1982, 603–613.

———. (1985) Jumping and leaping. Pp. 58–72 *in* M. Hildebrand, D. M. Bramble, K. F. Liem, and D. B. Wake, eds. Functional vertebrate morphology. Belknap Press, Cambridge, MA.

Fabrezi, M. (2006) Morphological evolution of Ceratophryinae (Anura, Neobatrachia). *J. Zool. Syst. Evol. Res*, 44, 153–166.

Gomez, C., Özbudak, E.M., Wunderlich, J., Baumann, D., Lewis, J. & Pourquié, O. (2008) Control of segment number in vertebrate embryos. *Nature*, 454, 335–339.

Gower, J.C. (1975) Generalized Procrustes analysis. *Psychometrika*, 40, 33–51.

Griffiths, I. (1963) The phylogeny of the Salientia. *Biol. Rev.*, 38, 241–292.

Haas, A. (1999) Larval and metamorphic skeletal development in the fast-developing frog *Pyxicephalus adspersus* (Anura, Ranidae). *Zoomorphology*, 119, 23–35.

Hall, B.K. (1995) Homology and embryonic development. *Evol. Biol.*, 28, 1–37.

Handrigan, G.R. & Wassersug, R.J. (2007) The anuran Bauplan: a review of the adaptive, developmental, and genetic underpinnings of frog and tadpole morphology. *Biol. Rev. Camb. Philos. Soc.*, 82, 1–25.

Hoff, K.V.S. & Wassersug, R.J. (2000) Tadpole locomotion: axial movement and tail functions in a largely vertebraeless vertebrate. *Am. Zool.*, 40, 62–76.

Iijima, M. & Kubo, T. (2019) Comparative morphology of presacral vertebrae in extant crocodylians: taxonomic, functional and ecological implications. *Zool. J. Linn. Soc.*, 186, 1006–1025.

IUCN. (2021) The IUCN Red List of Threatened Species. Version 2021–2.

Jones, K.E. (2015) Evolutionary allometry of lumbar shape in Felidae and Bovidae. *Biol. J. Linn. Soc. Lond.*, 116, 721–740.

Jones, K.E. & Pierce, S.E. (2016) Axial allometry in a neutrally buoyant environment: effects of the terrestrial-aquatic transition on vertebral scaling. *J. Evol. Biol.*, 29, 594–601.

Jones, K.E., Angielczyk, K.D., Polly, P.D., Head, J.J., Fernandez, V., Lungmus, J.K., Tulga, S. & Pierce, S.E. (2018a) Fossils reveal the complex evolutionary history of the mammalian regionalized spine. *Science*, 361, 1249–1252.

Jones, K.E., Benitez, L., Angielczyk, K.D. & Pierce, S.E. (2018b) Adaptation and constraint in the evolution of the mammalian backbone. *BMC Evol. Biol.*, 18, 172.

Keeffe, R. & Blackburn, D.C. (2020) Comparative morphology of the humerus in forward-burrowing frogs. *Biol. J. Linn. Soc. Lond.*, 131, 291–303.

Long, J.H., Jr., Pabst, D.A., Shepherd, W.R. & McLellan, W.A. (1997) Locomotor design of dolphin vertebral columns: bending mechanics and morphology of *Delphinus delphis*. *J. Exp. Biol.*, 200, 65–81.

Maglia, A.M. (1998) Phylogenetic relationships of extant pelobatoid frogs (Anura: Pelobatoidea): evidence from adult morphology. *Sci. Pap. Univ. Kansas. Nat. Hist. Mus.*, 10, 1–19.

Marchesi, M.C., Mora, M.S., Dans, S.L. & González-José, R. (2021) Allometry and ontogeny in the vertebral column of southern hemisphere dolphins: a 3D morphofunctional approach. *J. Mamm. Evol.*, 28, 125–134.

María, G.P. (2001) Skeletal development of *Leptodactylus chaquensis* (Anura: Leptodactylidae). *Herpetologica*, 57, 318–335.

Matojo, N.D. (2015) Rastapodidae fam. nov. of "Harrowfoot Frogs" (Anura: Neobatrachia) inferred from *Breviceps mossambicus* re-description (formerly in Brevicipitidae) from Tanzania. *J. Biol. Nat.*, 4, 200–205.

Maxwell, E.E., Romano, C. & Wu, F.X. (2021) Regional disparity in the axial skeleton of Saurichthyidae and implications for axial regionalization in non-teleostean actinopterygians. *J. Zool.*, 315, 29–41.

McCranie, J.R. & Castañeda, F.E. (2005) The herpetofauna of Parque Nacional Pico Bonito, Honduras. *Phyllomedusa: J. Herpetol.*, 4, 3–16.

Moen, D.S. (2019) What determines the distinct morphology of species with a particular ecology? The roles of many-to-one mapping and trade-offs in the evolution of frog ecomorphology and performance. *Am. Nat.*, 194, E81–E95.

Moen, D.S. & Wiens, J.J. (2017) Microhabitat and climatic niche change explain patterns of diversification among frog families. *Am. Nat.*, 190, 29–44.

Moen, D.S., Irschick, D.J. & Wiens, J.J. (2013) Evolutionary conservatism and convergence both lead to striking similarity in ecology, morphology and performance across continents in frogs. *Proc. R. Soc. B Biol. Sci.*, 280, 20132156.

Moen, D.S., Morlon, H. & Wiens, J.J. (2016) Testing convergence versus history: convergence dominates phenotypic evolution for over 150 million years in frogs. *Syst. Biol.*, 65, 146–160.

Molnar, J.L., Pierce, S.E., Bhullar, B.-A.S., Turner, A.H. & Hutchinson, J.R. (2015) Morphological and functional changes in the vertebral column with increasing aquatic adaptation in crocodylomorphs. *R Soc. Open Sci.*, 2, 150439.

Mookerjee, H.K. & Das, S.K. (1939) Further investigation on the development of the vertebral column in Salientia (Anura). *J. Morph.*, 64, 167–209.

Moran, N.A. (1994) Adaptation and constraint in the complex life cycles of animals. *Annu. Rev. Ecol. Syst.*, 25, 573–600.

Müller, J., Scheyer, T.M., Head, J.J., Barrett, P.M., Werneburg, I., Ericson, P.G.P., Pol, D. & Sánchez-Villagra, M.R. (2010) Homeotic effects, somitogenesis and the evolution of vertebral numbers in recent and fossil amniotes. *Proc. Natl. Acad. Sci. USA*, 107, 2118–2123.

Narita, Y. & Kuratani, S. (2005) Evolution of the vertebral formulae in mammals: a perspective on developmental constraints. *J. Exp. Zool. B Mol. Dev. Evol.*, 304, 91–106.

Nicholls, G.E. (1916) The structure of the vertebral column in the Anura Phaneroglossa and its importance as a basis of classification. *Proc. Linn. Soc. Lond.*, 28, 80–92.

Noble, G.K. (1922) The phylogeny of the Salientia: 1. The Osteology and the thigh musculature: their bearing on classification and phylogeny. American Museum of Natural History, New York.

Oliveira, B.F., São-Pedro, V.A., Santos-Barrera, G., Penone, C. & Costa, G.C. (2017) AmphiBIO, a global database for amphibian ecological traits. *Sci. Data*, 4, 170123.

Pereyra, M.O., Womack, M.C., Barrionuevo, J.S., Blotto, B.L., Baldo, D., Targino, M., Ospina-Sarria, J.J., Guayasamin, J.M., Coloma, L.A., Hoke, K.L., et al. (2016) The complex evolutionary history of the tympanic middle ear in frogs and toads (Anura). *Sci. Rep.*, 6, 34130.

Pourquié, O. (2003) The segmentation clock: converting embryonic time into spatial pattern. *Science*, 301, 328–330.

———. (2011) Vertebrate segmentation: from cyclic gene networks to scoliosis. *Cell*, 145, 650–663.

Pramuk, J.B. (2002) Combined evidence and cladistic relationships of West Indian toads (Anura: Bufonidae). *Herpetol. Monogr.*, 16, 121–151.

———. (2006) Phylogeny of south American Bufo (Anura: Bufonidae) inferred from combined evidence. *Zool. J. Linn. Soc.*, 146, 407–452.

Pugener, L.A. (2002). The vertebral column and spinal nerves of anurans. University of Kansas.

Pugener, L.A. & Maglia, A.M. (2009) Skeletal morphogenesis of the vertebral column of the miniature hylid frog *Acris crepitans*, with comments on anomalies. *J. Morph.*, 270, 52–69.

Pyron, R.A. (2014) Biogeographic analysis reveals ancient continental vicariance and recent oceanic dispersal in amphibians. *Syst. Biol.*, 63, 779–797.

Ram, K. & Wickham, H. (2018) wesanderson: a Wes Anderson palette generator. R package.

Randau, M. & Goswami, A. (2017) Morphological modularity in the vertebral column of Felidae (Mammalia, Carnivora). *BMC Evol. Biol.*, 17, 133.

———. (2018) Shape covariation (or the lack thereof) between vertebrae and other skeletal traits in felids: the whole is not always greater than the sum of parts. *Evol. Biol.*, 45, 196–210.

Randau, M., Goswami, A., Hutchinson, J.R., Cuff, A.R. & Pierce, S.E. (2016) Cryptic complexity in felid vertebral evolution: shape differentiation and allometry of the axial skeleton. *Zool. J. Linn. Soc.*, 178, 183–202.

Randau, M., Cuff, A.R., Hutchinson, J.R., Pierce, S.E. & Goswami, A. (2017) Regional differentiation of felid vertebral column evolution: a study of 3D shape trajectories. *Org. Divers. Evol.*, 17, 305–319.

Rawls, A. & Fisher, R.E. (2018) Developmental and functional anatomy of the spine. Pp. 1–29 *in* K. Kusumi and S. L. Dunwoodie, eds. The genetics and development of scoliosis. Springer International Publishing, Cham, Switzerland.

R Core Team. (2021) R: a language and environment for statistical computing. R Foundation for Statistical Computing, Vienna.

Reidenberg, J.S. (2007) Anatomical adaptations of aquatic mammals. *Anat. Rec.*, 290, 507–513.

Ritland, R.M. (1955) Studies on the post-cranial morphology of *Ascaphus truei*. I. Skeleton and spinal nerves. *J. Morph.*, 97, 119–177.

Rohlf, F.J. & Slice, D.E. (1990) Extensions of the Procrustes method for the optimal superimposition of landmarks. *Syst. Zool.*, 39, 40–59.

Sadier, A., Sear, K.W. & Womack, M. (2022) Unraveling the heritage of lost traits. *J. Exp. Zool. B Mol. Dev. Evol.*, 338, 107–118.

Schilling, N. (2011) Evolution of the axial system in craniates: morphology and function of the perivertebral musculature. *Front. Zool.*, 8, 4.

Stepanova, N. & Womack, M.C. (2020) Anuran limbs reflect microhabitat and distal, later-developing bones are more evolutionarily labile. *Evolution*, 74, 2005–2019.

Vidal-García, M. & Keogh, J.S. (2017) Phylogenetic conservatism in skulls and evolutionary lability in limbs – morphological evolution across an ancient frog radiation is shaped by diet, locomotion and burrowing. *BMC Evol. Biol.*, 17, 1–15.

Wickham, H. (2016) ggplot2: elegant graphics for data analysis. Springer-Verlag, New York.

Wild, E.R. (1999) Description of the chondrocranium and osteogenesis of the Chacoan burrowing frog, *Chacophrys pierotti* (Anura: Leptodactylidae). *J. Morphol.*, 242, 229–246.

Zhang, M., Zhu, W., Wang, B., Wang, S., Chang, L., Zhao, T. & Jiang, J. (2021) Osteological development of a small and fast metamorphic frog, *Microhyla fissipes* (Anura, Neobatrachia, Microhylidae). *J. Anat.*, 239, 1318–1335.

Zweifel, R.G., Clark, J., Alexander, A.M. & Kellogg, L.P. (1956) Two pelobatid frogs from the Tertiary of North America and their relationships to fossil and Recent forms. *Am. Mus. Novit.*, 1762, 1–45.

Associate Editor: Brian L. Sidlauskas
Handling Editor: Miriam L. Zelditch

Supporting Information

Additional supporting information may be found online in the Supporting Information section at the end of the article.

Table S1. Specimen information and species data.

Table S1. Specimen information and species data.